

## Characterization of bitumen modified with pyrolytic carbon black from scrap tires

Wang, Haopeng; Lu, Guoyang; Feng, Shuyin; Wen, Xiaobo; Yang, Jun

**DOI**

[10.3390/su11061631](https://doi.org/10.3390/su11061631)

**Publication date**

2019

**Document Version**

Final published version

**Published in**

Sustainability

**Citation (APA)**

Wang, H., Lu, G., Feng, S., Wen, X., & Yang, J. (2019). Characterization of bitumen modified with pyrolytic carbon black from scrap tires. *Sustainability*, 11(6), Article 1631. <https://doi.org/10.3390/su11061631>

**Important note**

To cite this publication, please use the final published version (if applicable).  
Please check the document version above.

**Copyright**

Other than for strictly personal use, it is not permitted to download, forward or distribute the text or part of it, without the consent of the author(s) and/or copyright holder(s), unless the work is under an open content license such as Creative Commons.

**Takedown policy**

Please contact us and provide details if you believe this document breaches copyrights.  
We will remove access to the work immediately and investigate your claim.

## Article

# Characterization of Bitumen Modified with Pyrolytic Carbon Black from Scrap Tires

Haopeng Wang <sup>1,\*</sup>, Guoyang Lu <sup>2,\*</sup>, Shuyin Feng <sup>3</sup>, Xiaobo Wen <sup>4</sup> and Jun Yang <sup>5</sup>

<sup>1</sup> Section of Pavement Engineering, Faculty of Civil Engineering and Geosciences, Delft University of Technology, Stevinweg 1, 2628 CN Delft, The Netherlands

<sup>2</sup> Institute of Highway Engineering, RWTH Aachen University, 52074 Aachen, Germany

<sup>3</sup> Department of Civil Engineering, University of Bristol, Bristol BS8 1TR, UK; shuyin.feng@bristol.ac.uk

<sup>4</sup> JSTI Group, Nanjing 211112, China; wxb168@jsti.com

<sup>5</sup> School of Transportation, Southeast University, Nanjing 211189, China; yangjun@seu.edu.cn

\* Correspondence: haopeng.wang@tudelft.nl (H.W.); lu@isac.rwth-aachen.de (G.L.); Tel.: +31-062-536-1801 (H.W.)

Received: 27 February 2019; Accepted: 14 March 2019; Published: 18 March 2019



**Abstract:** Pyrolytic carbon black (CB<sub>p</sub>) from scrap tire pyrolysis is a potential modifier for the bitumen industry. Binders containing different contents of CB<sub>p</sub> were prepared and experimentally investigated to examine the effects of CB<sub>p</sub> on the electrical and thermal conductivity, conventional physical properties, rheological properties, high-temperature antirutting performance, aging resistance, and storage stability. Laboratory test results indicated that the incorporation of CB<sub>p</sub> effectively improves the electrothermal properties, rheological properties, high-temperature rutting resistance, and aging resistance. It also increases the viscosity and decreases the storage stability of bitumen. The study confirms that CB<sub>p</sub>-modified bitumen with proper selection of content can be a multifunctional paving material.

**Keywords:** bitumen; carbon black; rheological property; electrical conductivity; storage stability; scrap tire pyrolysis

---

## 1. Introduction

With the transport development and the associated increase in numbers of vehicles, an estimated one billion (~17 million tons) end-of-life tires (ELTs) are generated every year worldwide [1]. This number has been growing steadily and this trend is expected to continue in the future. The countries of the European Union (EU), the USA, China, Japan, and India produce the largest amounts of scrap tires, accounting for almost 88% of the gross around the world. The illegally dumped or stockpiled tires pose a potential threat to both human health and environmental issues [2]. The rising environmental awareness and economic benefits have driven people to seek sustainable treatment and disposal of ELTs, such as retreading, energy recovery, pyrolysis, and material recycling [3,4]. Typical applications of recycled scrap tires in civil engineering practice include (i) rubber modified asphalt pavements, (ii) flooring for playgrounds and sports fields, (iii) highway crash barriers, dock bumpers and artificial reefs, (iv) roofing materials, etc. [5,6].

From a materials point of view, scrap tires are still a valuable source of raw materials in other applications. In general, the tire is made of rubber/elastomer, carbon black, metal, and other processing additives. The recycled rubber has been successfully utilized in paving industry for several decades due to the tremendous advantages. However, carbon black, which is used as a reinforcing filler and antioxidant of rubber, has not gained sufficient attention in the modification of bitumen. Although the properties of crumb rubber modified bitumen, where the crumb rubber usually contains carbon black, have been investigated for a long time, the individual effect of carbon black on the modification of

bitumen is still not very clear. Carbon black possesses many unique properties that distinguish it from other conventional fillers. Carbon black usually has a large specific surface area and irregular shapes. The surface of carbon black is also reported to have various functional groups [7]. Moreover, it is often added to different composite materials to enhance their electrical and thermal conductivities [8,9]. The unique physiochemical properties of carbon black make itself a promising and multifunctional modifier of the bitumen [10]. This study investigated the various properties of bitumen modified with the pyrolytic carbon black (CB<sub>p</sub>), a by-product from scrap tire pyrolysis. The present study not only helps the understanding of the role of carbon black in crumb rubber modified bitumen, but also explores the possibility to incorporate carbon black into bitumen as an independent modified binder. To examine the modification effect of pyrolytic carbon black on bitumen, the electrical resistivity, thermal conductivity, conventional physical properties, rheological properties, high-temperature antirutting performance, aging resistance, and storage stability were investigated by various laboratory tests.

## 2. Materials and Methods

### 2.1. Materials

The neat bitumen used in this study was SH-70, provided by Jiangsu Baoli Asphalt Co., LTD (Jiangyin, China). The basic properties of SH-70 are listed in Table 1. Pyrolytic carbon black (CB<sub>p</sub>) was obtained by vacuum pyrolysis of scrap tires at a total pressure of 20 kPa and a temperature of 480–520 °C from Henan Yinggo Technology Co, Ltd. (Henan, China). The technical information about CB<sub>p</sub> is listed in Table 2.

**Table 1.** Basic properties of neat bitumen SH-70.

Properties	Unit	Value
Penetration (25 °C, 100 g, 5 s)	dmm	71
Ductility (5 cm/min, 5 °C)	cm	32.2
Softening point (R&B)	°C	47.5
Flash point	°C	272
Rotational viscosity (60 °C)	Pa·s	203
Wax content	%	1.6
Density (15 °C)	g/cm <sup>3</sup>	1.032

**Table 2.** Basic properties of pyrolytic carbon black.

Properties	Unit	Value
Iodine absorption	g/kg	82
DPB absorption	cm <sup>3</sup> /100 g	102
DPB absorption of the compressed sample	cm <sup>3</sup> /100 g	90
CTAB surface area	cm <sup>2</sup> /100 g	83
Nitrogen absorption surface area	cm <sup>2</sup> /100 g	79
Heating loss	%	2.3
Ash content	%	0.3
Density	g/cm <sup>3</sup>	1.871
45-μm sieve residue	%	0.09
Tensile modulus at 300% strain	MPa	1.8
Electrical resistivity	Ω·cm	0.472

### 2.2. Sample Preparation

All CB<sub>p</sub> modified bitumen (CMB) samples were prepared using the high shear process. The neat bitumen was firstly heated to 150 °C and continuously stirred. Then it was mixed with CB<sub>p</sub> at various contents (3%, 6%, 9%, 12%, 15%, and 18% by weight of the neat bitumen). The blend was then mixed at 150 °C for 1 h using a high-speed shear mixer at a rate of 2000 rpm. The prepared binders with different CB<sub>p</sub> contents were designated as CMB-3, CMB-6, CMB-9, CMB-12, CMB-15, and CMB-18.

### 2.3. Testing Methods

#### 2.3.1. Electrical Resistivity and Thermal Conductivity Measurement

The electrical resistivity of bitumen was measured on a disk specimen of 25 mm diameter and 1 mm height, which corresponds to the geometry of specimen used in the dynamic shear rheometer tests. The resistivity of specimens was measured by the two-probe method. To minimize contact resistivity, silver paint, in conjunction with a copper plate, was used for the electrical contact with both ends of the circular plate specimen. A UNI-T modern digital multimeter (Dongguan, China) was connected with the copper electrodes to measure the resistivity of bitumen. The test temperature is 20 °C. The electric field of the multimeter is assumed constant and the end-effects are considered negligible. The steps of specimen preparation and measurement of electrical resistivity are shown in Figure 1.

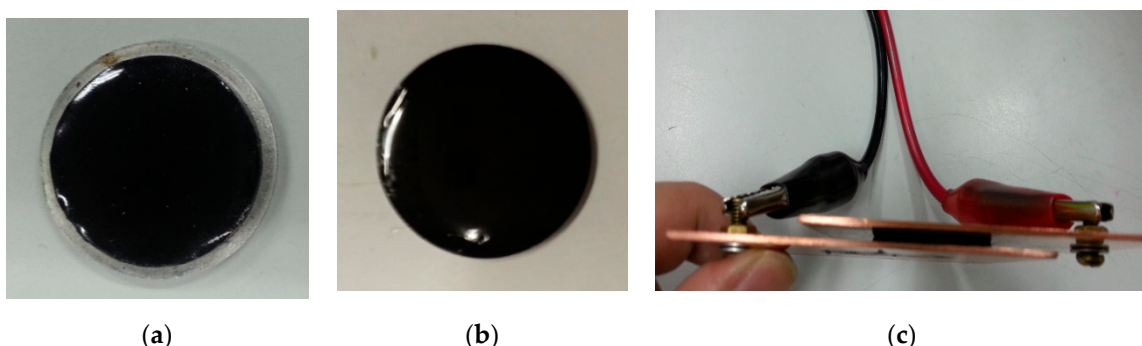


**Figure 1.** Electrical resistivity measurement process: (a) specimen molding; (b) specimen demolding; and (c) electrodes connecting with specimen.

From the resistivity readings of multimeter, the electrical resistivity of sample can be calculated based on Ohm's second law:

$$\rho = \frac{RS}{L} \quad (1)$$

where  $\rho$  is the electrical resistivity ( $\Omega \cdot \text{m}$ ),  $L$  is the internal electrode distance (m),  $S$  is the electrode conductive area ( $\text{m}^2$ ), and  $R$  is the measured resistivity ( $\Omega$ ).

The thermal conductivity of bitumen was measured by the advanced C-Therm TCi thermal analyzer (New Brunswick, Canada). The schematic diagram of the measuring system was shown in Figure 2. It comprises of a one-sided interfacial heat reflectance sensor, a sample cell with guard ring, a control unit, and a data acquisition unit. The prepared bitumen material was poured in a flat conical mold. The modified transient plane source (MTPS) method was employed by the TCi system for measuring the thermal conductivity. A known current is applied to the sensor's spiral heating element to provide a small amount of heat to the sample. By monitoring the change in the voltage drop of the sensor element, which is induced by the rise in temperature at the interface between the sensor and sample, the thermal properties of the sample can be determined. With the known heat flux and temperature gradient through the sample, the thermal conductivity can be calculated by Fourier's law:

$$q = -k \cdot \frac{dT}{dx} \quad (2)$$

where  $q$  is the heat flux density ( $\text{W}/\text{m}^2$ ),  $dT/dx$  is the temperature gradient ( $\text{K}/\text{m}$ ), and  $k$  is the thermal conductivity ( $\text{W}/\text{m} \cdot \text{K}$ ).

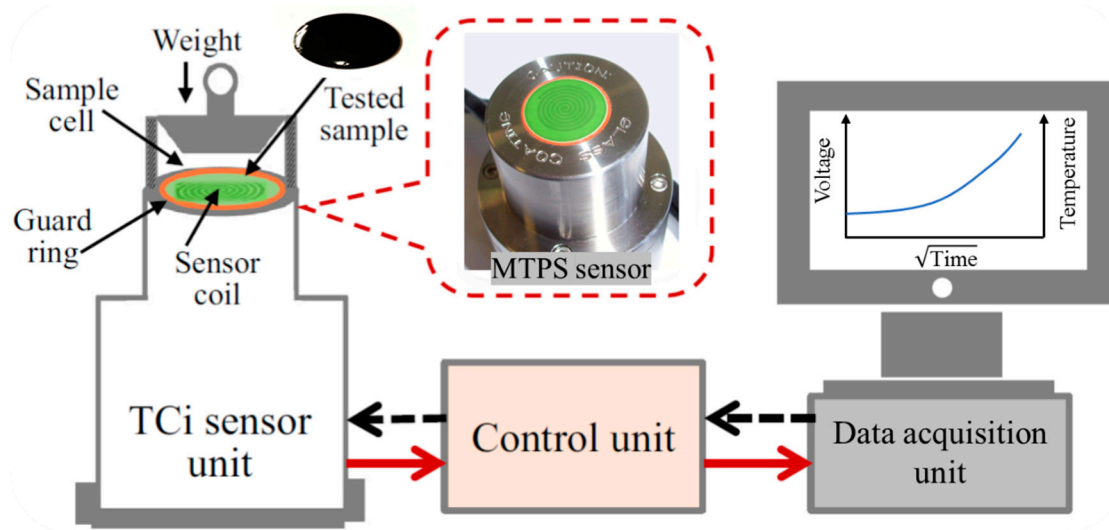


Figure 2. Schematic diagram of C-Therm TCi thermal conductivity analyzer [11].

### 2.3.2. Physical, Rheological, and Mechanical Properties Tests

Conventional physical properties of bituminous binders were studied by softening point test, penetration test and ductility test. A rotational viscometer (RV) was used to determine the dynamic viscosity of binders in the high-temperature range of production, transport, and construction. During the measurement, constant rotational speed (20 rpm) of the cylindrical spindle was maintained to monitor the torque at 135 °C and 165 °C.

The conventional binder tests, with simplistic indexes, only give an empirical representation of a material's rheological properties. Bitumen is a temperature- and time-dependent (i.e., the rate of loading), viscoelastic material. To have a better understanding of the viscoelastic behaviors, the rheological properties of each binder were also determined using a dynamic shear rheometer (DSR) following AASHTO T315-12. The parallel plate configuration with a diameter of 25 mm and a gap of 1 mm was used during the test.

Temperature sweep tests with 6 °C increments were applied to obtain the principle rheological parameters, complex modulus ( $G^*$ ) and phase angle ( $\delta$ ) at various temperatures. Typically, an angular frequency of 10 rad/s, which simulates the shear loading corresponding to a traffic speed of approximately 90 km/h, was applied.

The Multiple Stress Creep and Recovery (MSCR) test conducted on a DSR was utilized to investigate the high-temperature performance of bitumen. Two stress levels (0.1 kPa and 3.2 kPa) at 64 °C were applied on the sample according to AASHTO T350-14. The test protocol includes a 1-s creep load followed by a 9-s recovery at zero load in each cycle. Ten creep and recovery cycles were performed at each stress level. Two important parameters—the nonrecoverable creep compliance ( $J_{nr}$ ) and the percentage of recovery—were calculated to characterize the stress dependence and elastic response of bituminous binders.

### 2.3.3. Aging Procedure

The rolling thin film oven test (RTFOT) was used to simulate the short-term aging of bitumen according to ASTM D2872. The oven was kept at 163 °C for 85 min with the carriage rotating at a rate of 15 rpm. A pressure aging vessel (PAV) was used to simulate the long-term aging of bitumen. The short-term aged bitumen samples were subjected to the PAV at an aging temperature of 100 °C and an air pressure of 2.1 MPa for 20 h.

### 2.3.4. Storage Stability Test

The hot storage stability of binders was evaluated by the “tube test” according to ASTM D7173. In this test, an aluminum foil tube with standard dimensions (25 mm in diameter and 140 mm in height) was poured with the binder sample ( $50 \pm 0.5$  g) with due precaution to avoid the incorporation of air bubbles. The tubes were kept in an oven vertically at  $163 \pm 5$  °C for  $48 \pm 1$  h. Then, the tubes were moved to the refrigerator and cooled to  $-10 \pm 2$  °C. After cooling, the tubes were cut into three equal parts. Samples from the top, middle, and bottom parts of the tube were collected and stored for further testing.

## 3. Results and Discussion

### 3.1. Electrothermal Properties

It was reported the addition of carbon black can enhance the electrothermal properties of various composites [8,9]. It is also of much interest to see how it influences the electrothermal properties of bitumen since the concept of conductive asphalt pavement becomes more and more popular in functional pavement design [12]. Usually bitumen and normal aggregates are considered insulators. The conductive asphalt mixture is achieved by adding conductive materials (such as carbon fiber, graphite, carbon black, steel fiber, etc.) into common asphalt mixtures [13–15]. To investigate the effect of pyrolytic carbon black on the electrothermal properties of bitumen, six carbon black contents (3%, 6%, 9%, 12%, 15%, and 18% by weight of neat bitumen) were involved in this study. The electrical resistivity of different binders measured with the two-probe method is displayed in Figure 3. The results indicate that when added relatively low contents of  $\text{CB}_p$ , the electrical resistivity of  $\text{CB}_p$  modified bitumen (CMB) is close to that of neat asphalt binder, exhibiting an insulating behavior. As the content of  $\text{CB}_p$  increases, the electrical resistivity is reduced. A dramatic decline in the resistivity takes place after a certain content of  $\text{CB}_p$  (12 wt % in this study) has been added. Twelve weight percent is usually regarded as the threshold as explained by the percolation theory [16]. After this percolation threshold, when continuously increasing the content of graphite, the electrical resistivity decreases slowly. Based on the graph, changes in the electrical resistivity under various  $\text{CB}_p$  contents can be roughly divided into three phases: (1) Insulated phase.  $\text{CB}_p$  particles are so isolated that there is not a valid conductive path formed for electrons within the bitumen sample. (2) Transition phase. More  $\text{CB}_p$  particles start to contact with each other and the valid conductive paths form. (3) Conductive phase. Occurs if the insulated phase ends with sufficiently low resistivity [17].

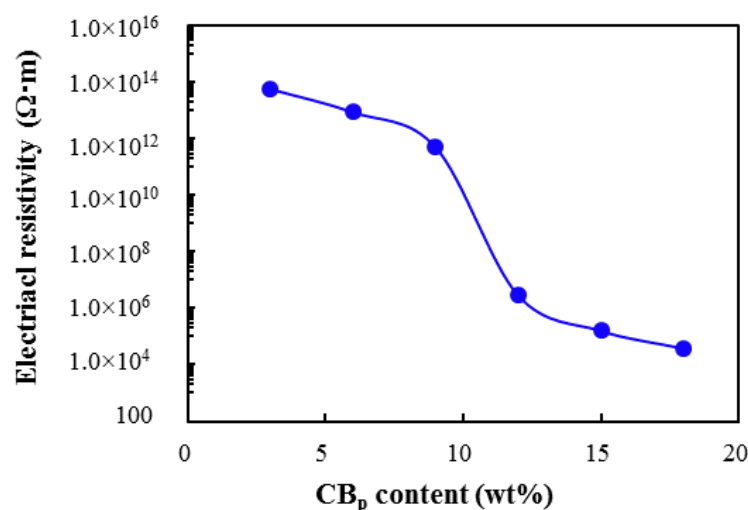


**Figure 3.** Electrical resistivity of bitumen with different contents of pyrolytic carbon black.

Similarly, the thermal conductivity of bitumen with different  $\text{CB}_p$  contents was also measured and is shown in Figure 4. It is obvious that the thermal conductivity of bitumen is increased continuously by the addition of  $\text{CB}_p$ . However, it shows a different pattern from the electrical resistivity curve. At the initial stage with low contents of  $\text{CB}_p$ , the thermal conductivity of CMB exhibits a linear increase with the continuous addition of  $\text{CB}_p$ . When the content of  $\text{CB}_p$  is beyond 9 wt %, the increasing trend of thermal conductivity is more significant. It is interesting to note that this transition point of  $\text{CB}_p$  content is similar to the content corresponding to the threshold value in the evolution of electrical resistivity. This is because  $\text{CB}_p$  particles begin to form conductive paths at ~9 wt %, and there is a change in the conductive system from the dispersed system (bitumen) to the attached system (pyrolytic carbon black), resulting in a rapid increase in thermal conductivity. However, the increase in thermal conductivity occurs less rapidly than electrical conductivity. The reason for this phenomenon is the electrical resistivity of  $\text{CB}_p$  ( $0.472 \Omega \cdot \text{cm}$ ) is much lower than that of bitumen (almost an insulator). Therefore, most of the electric current flows through the formed conductive  $\text{CB}_p$  paths instead of bitumen. On the other hand, because the thermal conductivity of  $\text{CB}_p$  is not significantly greater than that of bitumen, heat flows not only through the formed conductive  $\text{CB}_p$  paths, but also through the bitumen itself. Consequently, the thermal conductivity of CMB is less influenced than electrical resistivity by the exponential increase of the number of conductive paths [18]. In a summary, the enhanced electrothermal properties of CMB make it a promising multifunctional binder in asphalt pavement, such as snow melting, ice removing, energy harvesting, etc.

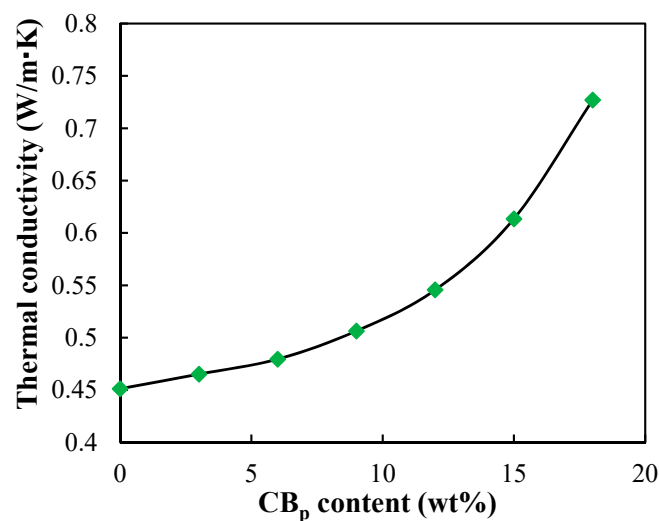


**Figure 4.** Thermal conductivity of bitumen with different contents of pyrolytic carbon black.

### 3.2. Conventional Physical Properties

The physical properties, including softening point, penetration, and ductility, of CMB with different  $\text{CB}_p$  contents are shown in Figure 5. The softening point reflects the viscosity of bitumen. Penetration indicates the degree of softness and consistency as well as the relative viscosity of bitumen. Ductility evaluates the tensile deformation and flexibility of bitumen. The results show that penetration and ductility values of CMB are all smaller than those of the neat bitumen, whereas the softening points of CMB are greater than that of neat bitumen. The effects mentioned above are strengthened with increasing contents of  $\text{CB}_p$ . The above analyses demonstrate that  $\text{CB}_p$  can improve on the high-temperature properties of CMB. It maybe attributes to the unique properties of  $\text{CB}_p$ , which has high oil absorption capability and surface area. This eventually leads to the absorption of most lightweight fractions of bitumen and hence stiffens it. In view of the consistent effects of  $\text{CB}_p$  content on the physical properties of bitumen, bitumen, with only three different  $\text{CB}_p$  contents (CMB-6, CMB-12, and CMB-18), was investigated in the further bitumen tests.

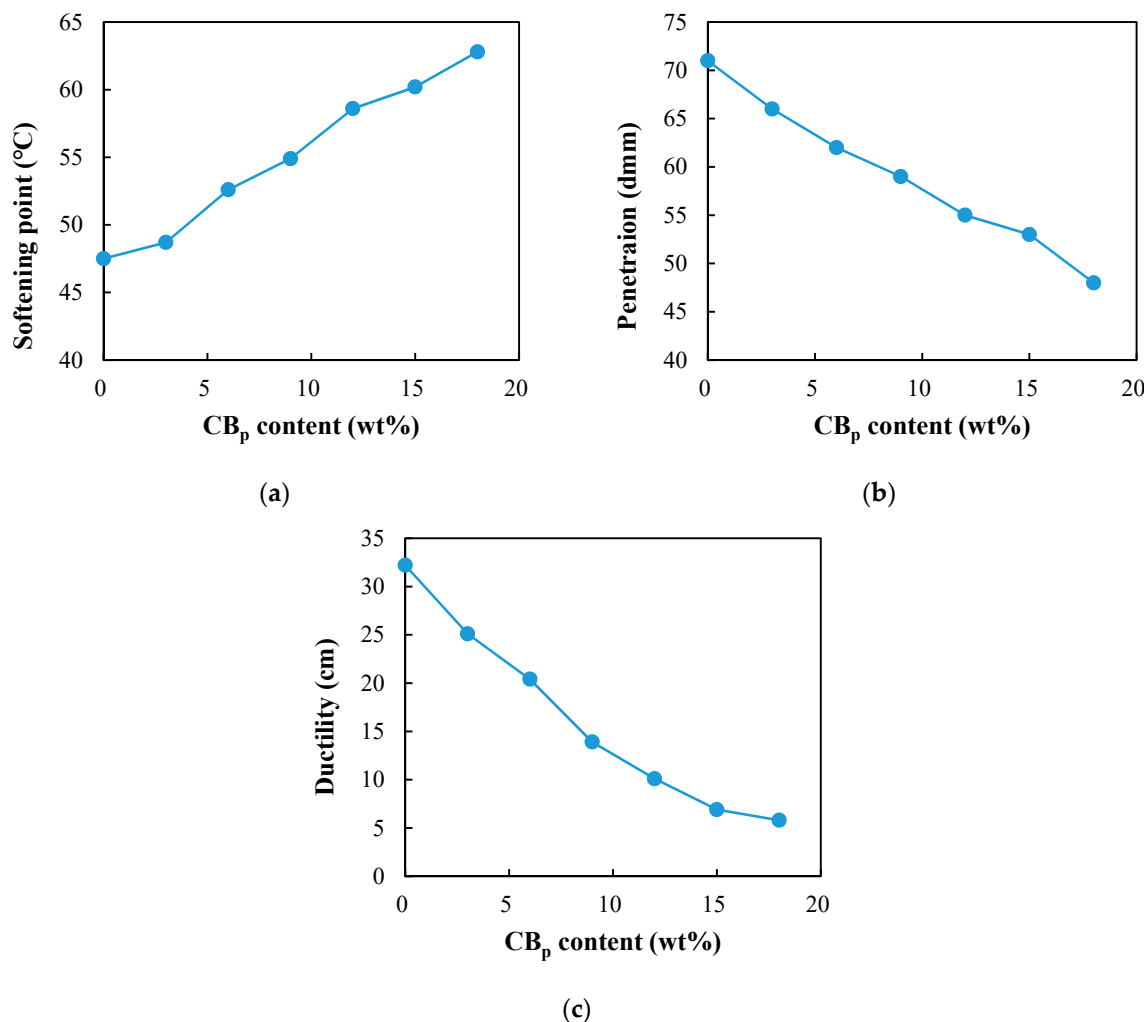


**Figure 5.** Conventional physical properties of bitumen with different contents of pyrolytic carbon black: (a) softening point; (b) penetration; and (c) ductility.

### 3.3. Rotational Viscosity

The flow characteristics of bituminous binders, which are crucial to the pumpability, mixability, and workability, can be characterized by viscosity [19]. Figure 6 presents the results of unaged binders obtained from rotational viscosity tests. As temperature increases from 135 to 165 °C, the viscosities of all binders decrease accordingly. Moreover, the addition of CB<sub>p</sub> significantly increases the binder viscosity. The more CB<sub>p</sub> content was added, the higher binder viscosity can be measured. In the paving industry, the viscosity–temperature relationship is built to determine the equiviscous temperature ranges for selecting suitable mixing and compaction temperatures for hot mix asphalt. The recommended viscosity ranges for mixing and compaction temperatures are  $0.17 \pm 0.02$  Pa·s and  $0.28 \pm 0.03$  Pa·s, respectively [20]. The viscosity values together with the determined mixing and compaction temperatures from the temperature–viscosity curves in Figure 6 are summarized in Table 3. With the increase of CB<sub>p</sub> content, the mixing and compaction temperatures of CMB should be increased accordingly to ensure the mixability and workability. However, these temperature ranges are still lower than that of the common polymer-modified bitumens.

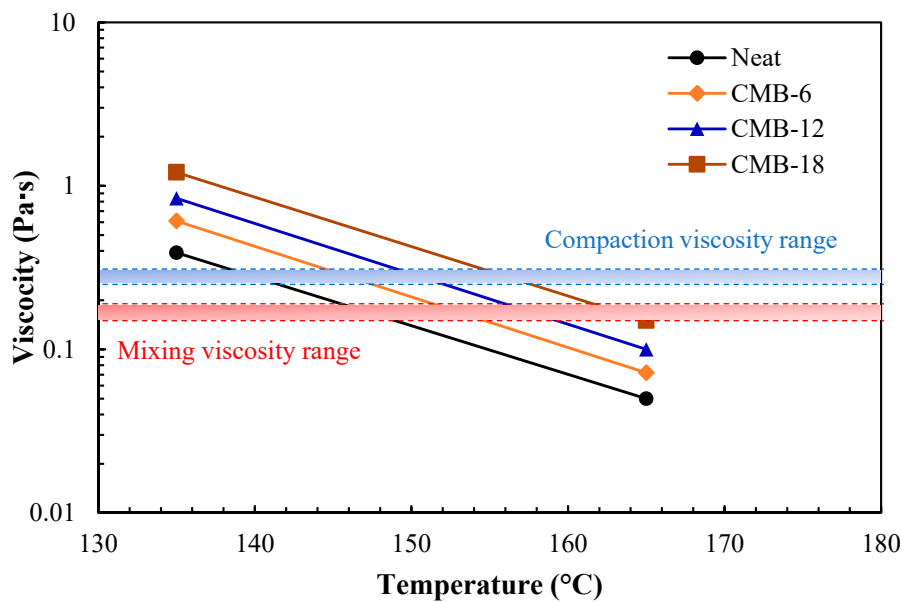


**Figure 6.** Rotational viscosity of bitumen with different contents of pyrolytic carbon black.

**Table 3.** Rotational viscosity values and determined mixing/compaction temperatures of different binders.

Binder Types	Rotational Viscosity (Pa·s)		Temperature Range (°C)	
	135 °C	165 °C	Mixing	Compaction
Neat bitumen	0.39	0.05	147–150	139–143
CMB-6	0.61	0.07	152–155	145–148
CMB-12	0.84	0.11	156–160	149–152
CMB-18	1.21	0.15	162–166	155–158

### 3.4. Rheological Properties

The complex shear modulus and phase angle of different binders were obtained from dynamic shear rheometer tests. Figure 7 shows the temperature dependence of complex modulus and phase angle at 10 rad/s for each binder in a temperature range from 52 to 82 °C. The results in Figure 7a indicate that the addition of  $CB_p$  increases the complex modulus of bitumen, which can be attributed to the stiffening effect of  $CB_p$  facilitated by the absorption of light fractions of bitumen. Moreover, the slope of the semilogarithmic curve of complex modulus versus temperature is gradually reduced with the increase of  $CB_p$  content. This means that CMB is less susceptible to temperature changes than neat bitumen. It can be seen from Figure 7b that  $CB_p$  decreases the phase angle of bitumen, making the material more elastic. This indicates CMB may have a better rutting resistance since it has more elastic recovery than the neat bitumen. However, the phase angles of the binders at the testing temperature range are all higher than 80°, which is still much higher than that of common polymer-modified bitumen [21]. The limited elastic recovery performance of CMB was also confirmed by the multiple stress creep recovery test.

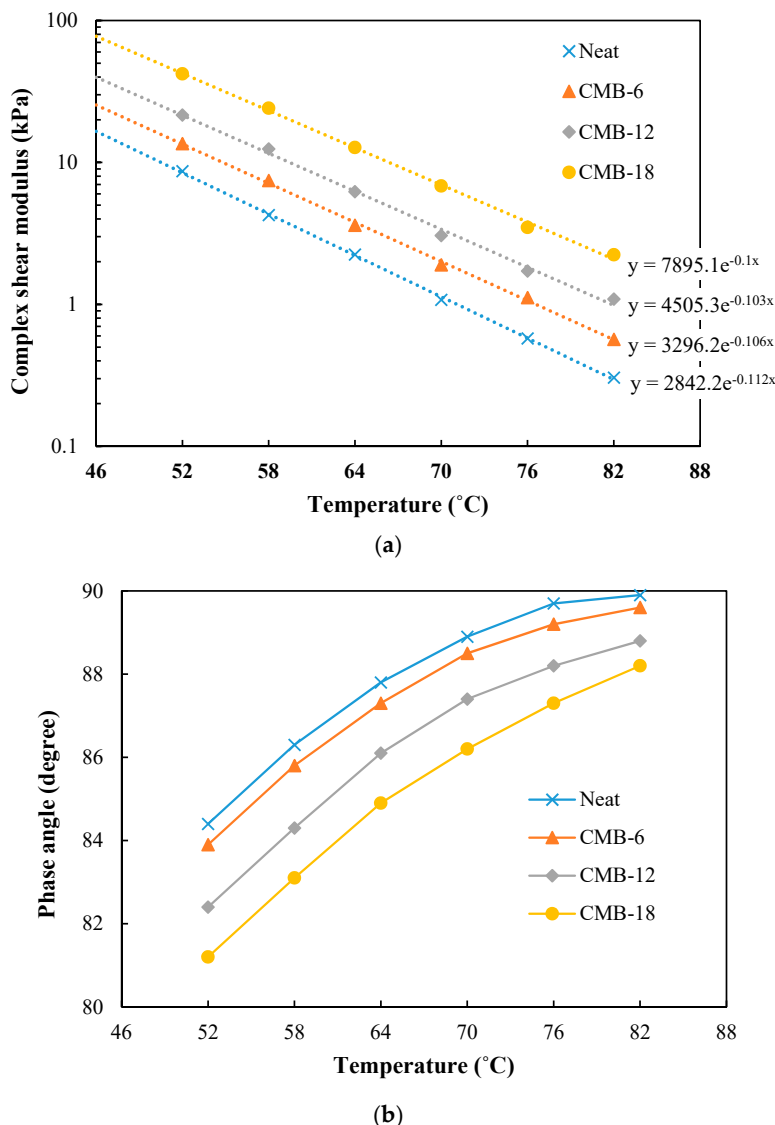


**Figure 7.** Rheological parameters of bitumen with different contents of pyrolytic carbon black at different temperatures: (a) complex shear modulus and (b) phase angle.

### 3.5. Multiple Stress Creep Recovery Test

MSCR tests were carried out to evaluate the rutting performance of binders at high temperatures. The nonrecoverable creep compliance and percentage of recovery of different binders at the stress level of 3.2 kPa are presented in Figure 8. The nonrecoverable creep compliance,  $J_{nr}$ , as opposed to the SHRP criteria,  $G^*/\sin \delta$ , provides a much better correlation to rutting [22]. Binders with lower  $J_{nr}$  values are considered to have better rutting resistance. It is clear that the incorporation of  $CB_p$  decreased the  $J_{nr}$  values of bitumen, indicating improved high-temperature rutting resistance. In addition, the percentage of recovery of bitumen was also increased due to the addition of  $CB_p$ , but only to a limited extent. This result coincides with the phase angle results from rheological tests.

To evaluate the aging properties, both short-term (RTFOT) and long-term aging (PAV) tests were conducted on bitumen samples to simulate the aging process during the stages of mixing and placement, and the stage of in service. The aged samples were subjected to the MSCR tests. By comparing the nonrecoverable creep compliance of bitumen before and after aging, the following aging index (AI) was defined.

$$AI = \frac{J_{nr, aged}}{J_{nr, unaged}} \quad (3)$$

where  $J_{nr, aged}$  is the nonrecoverable creep compliance of either RTFOT- or PAV-aged samples;  $J_{nr, unaged}$  is the nonrecoverable creep compliance of fresh bitumen. It is obvious that binder having an AI close to unity is assumed to be more aging resistant in this study. The aging indices of different binder samples are shown in Figure 9. Both RTFOT and PAV aging made the binder stiffer, exhibiting lower  $J_{nr}$  values. With the increase of  $CB_p$  content, the aging indices of bitumen at both aging states are higher and closer to unity. This obviously illustrates that the aging resistance of bitumen is significantly improved by the  $CB_p$  modification. This improvement is enhanced at higher contents of  $CB_p$ . There are possibly two reasons for the improved aging resistance of CMB. Firstly, the surface of  $CB_p$  is rich in various active functional groups that are more prone to react with oxygen than bitumen during the aging process. This in turn delays the oxidation aging of bitumen itself. Secondly, the  $CB_p$  is more compatible with the maltenes which are also partly absorbed during the dispersion process. It also creates a boundary layer (film) which is composed essentially of asphaltenes [23]. Since the aging of bitumen is mainly caused by the depletion of maltenes and the creation of more polar asphaltene-like substances, the existence of carbon black surrounded by asphaltene impedes the maltenes from aging. These two features of  $CB_p$  together contribute to improving the aging resistance of bitumen.

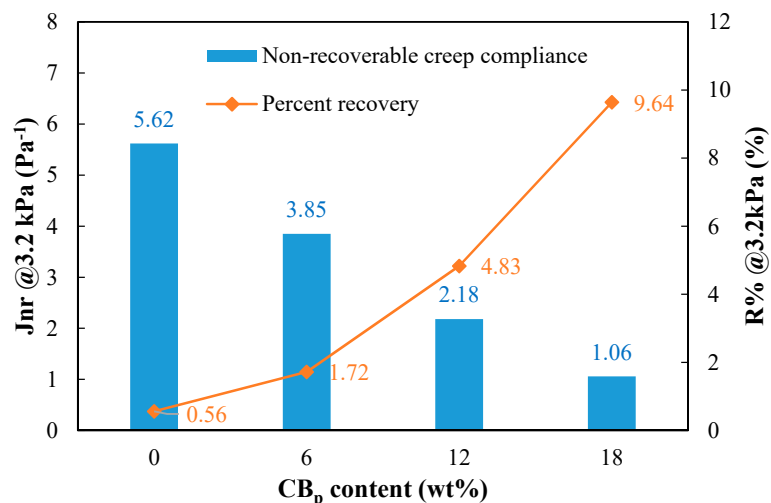


**Figure 8.** Multiple Stress Creep Recovery Test (MSCR) parameters of bitumen with different contents of pyrolytic carbon black at 64 °C.

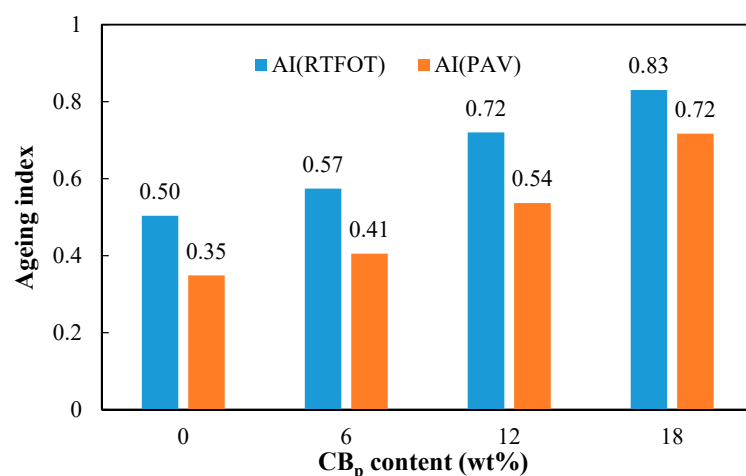


**Figure 9.** Effect of pyrolytic carbon black content on the aging properties of bitumen.

### 3.6. Hot-Temperature Storage Stability

To evaluate the storage stability of the samples, the stability index (SI) was developed by considering the property difference between bitumen samples from different parts of the tube. The  $J_{nr}$  values of the samples were used to calculate the SI in Equation (4).

$$SI = \frac{|J_{nr,t} - J_{nr,b}|}{J_{nr,avg}} \quad (4)$$

where  $J_{nr,t}$  and  $J_{nr,b}$  are the nonrecoverable compliances of the sample from the top and bottom parts in the tube, respectively.  $J_{nr,avg}$  is the averaged nonrecoverable compliance among the samples from the top, middle, and bottom parts; if the binder is absolutely homogenous and storage stable, the unit-less index SI should be zero. Therefore, a smaller SI value represents higher storage stability. Figure 10 shows the stability index of CMB with different  $CB_p$  contents. With the increase of  $CB_p$  content, the stability index of CMB increases, indicating lower storage stability. The effects of  $CB_p$  content on the storage stability of CMB binders can be explained by the Stoke's law [24]. This theory defines the terminal velocity ( $v_t$ ), which is the velocity of the displacement of the spherical particles when the gravity on the particles equals to the drag force (frictional force) on the particles in a Newtonian fluid in Equation (5). The phase separation in modified bitumen is governed by the terminal velocity of the dispersed phase (assumed as spherical particles) in a Newtonian fluid:

$$v_t = \frac{2}{9} \frac{r^2 \Delta \rho g}{\eta} \quad (5)$$

where  $r$  is the radius of the dispersed particle;  $\Delta \rho$  is the difference of density between the particle and Newtonian fluid medium;  $g$  is the gravitational acceleration; and  $\eta$  is the viscosity of the liquid medium. For CMB binders,  $CB_p$  particles are considered as the dispersed phase in the liquid bitumen medium. According to Equation (5), the terminal velocity of the particles is proportional to the square of the radius of dispersed particles and the density difference, and inversely related to the viscosity of the liquid medium. In the case of CMB,  $CB_p$  particles have a much higher density ( $1.871 \text{ g/cm}^3$ ) than bitumen ( $1.032 \text{ g/cm}^3$ ) and, consequently, have the tendency to settle down due to the gravitational force. One may argue that CMB with higher  $CB_p$  content has a higher viscosity which creates larger drag forces for the descending  $CB_p$  particles. Therefore, CMB at high  $CB_p$  content should be more stable than at low  $CB_p$  content. However, the terminal velocity in the Stoke's law only describes the speed of phase separation (or becoming unstable). It is not the driving force for phase separation to happen. Therefore, after sufficient conditioning time in the tube test, CMB with high  $CB_p$  content will have more distinctions among the different parts of the tube. This is eventually reflected by the higher stability index (less stable) in Figure 10.

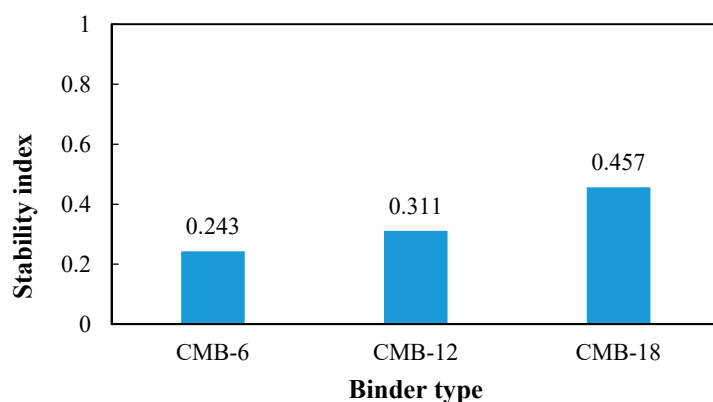


Figure 10. Effect of pyrolytic carbon black content on the storage stability of bitumen.

#### 4. Conclusions

From the various laboratory tests conducted on the pyrolytic carbon black modified bitumen binders, it can be concluded that pyrolytic carbon black is a promising modifier for bitumen modification. Specifically, it can enhance the electrothermal properties of bitumen, making the modified binder feasible for multifunctional applications. The enhancement mechanisms of electrical and thermal conductivity of bitumen by adding pyrolytic carbon black are different, resulting in different patterns in the evolution curves of conductivity versus pyrolytic carbon black content. The modification by pyrolytic carbon black increases the softening point and decreases penetration and ductility of the binder. Improved rheological properties were observed on the CMB binders, whose complex shear moduli are increased and phase angles are decreased. The temperature susceptibility is also reduced. The rutting resistance and aging resistance of bitumen are also improved by the incorporation of pyrolytic carbon black based on the MSCR test results.

Pyrolytic carbon black-modified bitumen binders have higher viscosities than neat bitumen, which means the mixing and compaction temperature windows need to be adjusted accordingly. The addition of pyrolytic carbon black into bitumen is detrimental to the storage stability of bitumen as most of the particulate matter modified bitumen. Cautions should be taken to find a suitable content of pyrolytic carbon black to ensure storage stability. Since the stiffening effect from modification usually contradicts the thermal cracking resistance, the low-temperature performance of CMB should also be addressed in the further studies. Future studies on the mixture level are recommended to examine the modification effect of pyrolytic carbon black on the paving applications.

**Author Contributions:** Conceptualization, H.W.; Formal Analysis, X.W.; Funding Acquisition, G.L. and X.W.; Investigation, G.L. and X.W.; Methodology, H.W. and S.F.; Project Administration, G.L. and J.Y.; Supervision, J.Y.; Writing—Original Draft, H.W.; Writing—Review and Editing, H.W. and S.F.

**Funding:** This research received no external funding.

**Acknowledgments:** The first author would like to acknowledge the scholarship from the China Scholarship Council.

**Conflicts of Interest:** The authors declare no conflict of interest.

#### References

1. WBCSD. *End-of-Life Tires: A Framework for Effective Management Systems*; World Business Council for Sustainable Development: Conches-Geneva, Switzerland, 2010.
2. Stevenson, K.; Stallwood, B.; Hart, A.G. Tire rubber recycling and bioremediation: A review. *Bioremediat. J.* **2008**, *12*, 1–11. [[CrossRef](#)]
3. Sienkiewicz, M.; Kucinska-Lipka, J.; Janik, H.; Balas, A. Progress in used tyres management in the European Union: A review. *Waste Manag.* **2012**, *32*, 1742–1751. [[CrossRef](#)] [[PubMed](#)]
4. Torretta, V.; Rada, E.C.; Ragazzi, M.; Trulli, E.; Istrate, I.A.; Cioca, L.I. Treatment and disposal of tyres: Two EU approaches. A review. *Waste Manag.* **2015**, *45*, 152–160. [[CrossRef](#)]
5. Lo Presti, D. Recycled tyre rubber modified bitumens for road asphalt mixtures: A literature review. *Constr. Build. Mater.* **2013**, *49*, 863–881. [[CrossRef](#)]
6. Wang, H.; Liu, X.; Apostolidis, P.; Scarpa, T. Review of warm mix rubberized asphalt concrete: Towards a sustainable paving technology. *J. Clean. Prod.* **2018**, *177*, 302–314. [[CrossRef](#)]
7. Roy, C.; Chaala, A.; Darmstadt, H. The vacuum pyrolysis of used tires—End-uses for oil and carbon black products. *J. Anal. Appl. Pyrol.* **1999**, *51*, 201–221. [[CrossRef](#)]
8. Huang, J.-C. Carbon black filled conducting polymers and polymer blends. *Adv. Polym. Technol.* **2002**, *21*, 299–313. [[CrossRef](#)]
9. Wen, S.H.; Chung, D.D.L. Effects of carbon black on the thermal, mechanical and electrical properties of pitch-matrix composites. *Carbon* **2004**, *42*, 2393–2397. [[CrossRef](#)]
10. Feng, Z.-G.; Rao, W.-Y.; Chen, C.; Tian, B.; Li, X.-J.; Li, P.-L.; Guo, Q.-L. Performance evaluation of bitumen modified with pyrolysis carbon black made from waste tyres. *Constr. Build. Mater.* **2016**, *111*, 495–501. [[CrossRef](#)]

11. Pal, A.; Thu, K.; Mitra, S.; El-Sharkawy, I.I.; Saha, B.B.; Kil, H.-S.; Yoon, S.-H.; Miyawaki, J. Study on biomass derived activated carbons for adsorptive heat pump application. *Int. J. Heat Mass Trans.* **2017**, *110*, 7–19. [[CrossRef](#)]
12. Pan, P.; Wu, S.P.; Xiao, F.P.; Pang, L.; Xiao, Y. Conductive asphalt concrete: A review on structure design, performance, and practical applications. *J. Intell. Mater. Syst. Struct.* **2015**, *26*, 755–769. [[CrossRef](#)]
13. Wang, H.; Yang, J.; Liao, H. Advances in self-monitoring asphalt concrete. In Proceedings of the 15th COTA International Conference of Transportation Professionals, Beijing, China, 24–27 July 2015; American Society of Civil Engineers: Reston, VA, USA, 2015; pp. 810–822.
14. Wang, H.; Yang, J.; Liao, H.; Chen, X. Electrical and mechanical properties of asphalt concrete containing conductive fibers and fillers. *Constr. Build. Mater.* **2016**, *122*, 184–190. [[CrossRef](#)]
15. Wang, H.; Yang, J.; Lu, G.; Liu, X. Accelerated healing in asphalt concrete via laboratory microwave heating. *J. Test. Eval.* **2020**, *48*. [[CrossRef](#)]
16. Wu, S.; Mo, L.; Shui, Z.; Chen, Z. Investigation of the conductivity of asphalt concrete containing conductive fillers. *Carbon* **2005**, *43*, 1358–1363. [[CrossRef](#)]
17. Cong, P.; Xu, P.; Chen, S. Effects of carbon black on the anti aging, rheological and conductive properties of sbs/asphalt/carbon black composites. *Constr. Build. Mater.* **2014**, *52*, 306–313. [[CrossRef](#)]
18. Agari, Y.; Uno, T. Thermal-conductivity of polymer filled with carbon materials—Effect of conductive particle chains on thermal-conductivity. *J. Appl. Polym. Sci.* **1985**, *30*, 2225–2235. [[CrossRef](#)]
19. Wang, H.; Liu, X.; Apostolidis, P.; Scarpas, T. Non-newtonian behaviors of crumb rubber-modified bituminous binders. *Appl. Sci.* **2018**, *8*, 1760. [[CrossRef](#)]
20. Wang, H.; Yang, J.; Gong, M. Rheological characterization of asphalt binders and mixtures modified with carbon nanotubes. In *Rilem Bookser*; Springer: Berlin/Heidelberg, Germany, 2016; pp. 141–150.
21. Airey, G. Rheological properties of styrene butadiene styrene polymer modified road bitumens. *Fuel* **2003**, *82*, 1709–1719. [[CrossRef](#)]
22. D’Angelo, J.A. The relationship of the mscr test to rutting. *Road Mater. Pavement Des.* **2011**, *10*, 61–80. [[CrossRef](#)]
23. Chaala, A.; Roy, C.; Ait-Kadi, A. Rheological properties of bitumen modified with pyrolytic carbon black. *Fuel* **1996**, *75*, 1575–1583. [[CrossRef](#)]
24. Ghavibazoo, A.; Abdelrahman, M.; Ragab, M. Effect of crumb rubber modifier dissolution on storage stability of crumb rubber-modified asphalt. *Trans. Res. Rec. J. Trans. Res. Board* **2013**, *2370*, 109–115. [[CrossRef](#)]



© 2019 by the authors. Licensee MDPI, Basel, Switzerland. This article is an open access article distributed under the terms and conditions of the Creative Commons Attribution (CC BY) license (<http://creativecommons.org/licenses/by/4.0/>).